ACSNANO

www.acsnano.org

ARTICLE

Water-Induced Self-Assembly of Amphiphilic Discotic Molecules for Adaptive Artificial Water Channels

Hsi-Yen Chang,[⊥] Kuan-Yi Wu,[⊥] Wei-Chun Chen, Jing-Ting Weng, Chin-Yi Chen, Ankit Raj, Hiro-o Hamaguchi, Wei-Tsung Chuang, Xiaosong Wang, and Chien-Lung Wang*

Cite This: *ACS Nano* 2021, 15, 14885−14890

Read Online

ACCESS | Metrics & More | Article Recommendations | Supporting Information

ABSTRACT: **Inspired by the induced-fit mechanism in nature, we developed the process of water-induced self-assembly (WISA) to make water an active substrate that regulates the self-assembly and function of amphiphilic discotic molecules (ADMs). The ADM is an isotropic liquid that self-assembles only when in contact with water. Characterization results indicate that water fits into the hydrophilic core of the ADMs and induces the formation of a hexagonal columnar phase (Col_h), where each column contains a hydrated artificial water channel (AWC). The hydrated AWCs are adaptive rather than static; the dynamic incorporation/removal of water results in the reversible assembly/disassembly of the adaptive AWCs (aAWCs). Furthermore, its dynamic characteristics can enable water to act as an orientation−directional guest molecule that controls the growth direction of the aAWCs. Well-aligned aAWC arrays that showed the ability of water transport were obtained *via* a "directional WISA" method. In WISA, water thus governs the supramolecular chemistry and function of synthetic molecules as it does with natural materials. By making water an active component in adaptive chemistry and enabling host molecules to dynamically interact with water, this adaptive aquatic material may motivate the development of synthetic molecules further toward biomaterials.**

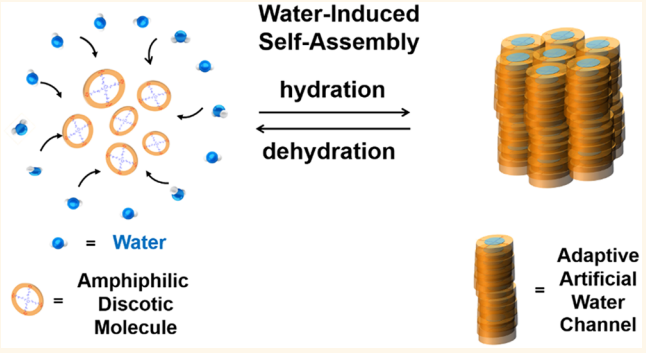

KEYWORDS: *supramolecular chemistry, induced-fit mechanism, adaptive self-assembly, artificial water channels, discotic liquid crystals, amphiphiles*

Downloaded via SYNCHROTRON RADIATION RESEARCH on February 16, 2022 at 05:44:32 (UTC).
See https://pubs.acs.org/sharingguidelines for options on how to legitimately share published articles.

Water, a major component in living creatures, has been found to act as an active substrate that operates microscopic motions such as the opening/closing, gating, and constricting[1−3] of biomolecules. These motions start from molecular recognition and can result in various physiological functions.[4−6] The process has been described by the well-accepted concept of the induced-fit mechanism, which is a kind of kinetic process where substrate molecules bind to host molecules and subsequently cause conformational changes to host molecules and carry out various functions. Examples such as transmembrane proteins perform biological functions based on the induced-fit mechanism. Some of these proteins are biological transporters that self-assemble into channel-like structures. Substrate molecules cause conformational changes of the transporters and activate the subsequent transport procedures. For example, glucose is the substrate that activates a sequence of protein conformational changes known as the "alternating conformation model", which facilitates glucose transport in or out of a cell.[7,8] A water molecule is the substrate that "opens" the hydrophobic gate of the ion transporters such as BEST1 and TMEM175[3,9] to enable the water/ion transport. Studies also show that structural damage[10] or changes in local flexibility[11] could prevent the substrate molecules from causing conformational changes, which consequently hinder the biological transporters from properly delivering their functions. The studies thus reveal the active role of substrate molecules in operating the self-assembly and functions of biomolecules.

In adaptive chemistry,[12,13] chemical effectors play a role similar to the substrate in an induced-fit mechanism. They are used to trigger the structural changes of synthetic molecules,

Received: June 11, 2021
Accepted: August 12, 2021
Published: August 19, 2021

© 2021 American Chemical Society

https://doi.org/10.1021/acsnano.1c04994
ACS Nano 2021, 15, 14885−14890

which activate the subsequent stimuli-responsiveness and biomimetic functions.[14−18] Water is also considered as a chemical effector in adaptive chemistry. It initiates self-healing of moisture-adaptive materials and provides hydrophobic interaction to self-assemble synthetic matters.[19−21] However, in these procedures, the synthetic matters can self-assemble and perform functions without water. Although water acts as the solvent to swell/aggregate the synthetic matters, it does not actively operate the self-assembly structures and functions of the synthetic matters as it operates the hydrophobic gates in the biological transporters.

Inspired by the induced-fit mechanism from nature, we developed the water-induced self-assembly (WISA) that uses water as the substrate to not only activate but also participate in the self-assembly and function of a synthetic host. The amphiphilic discotic molecule (ADM) as shown in Figure 1a

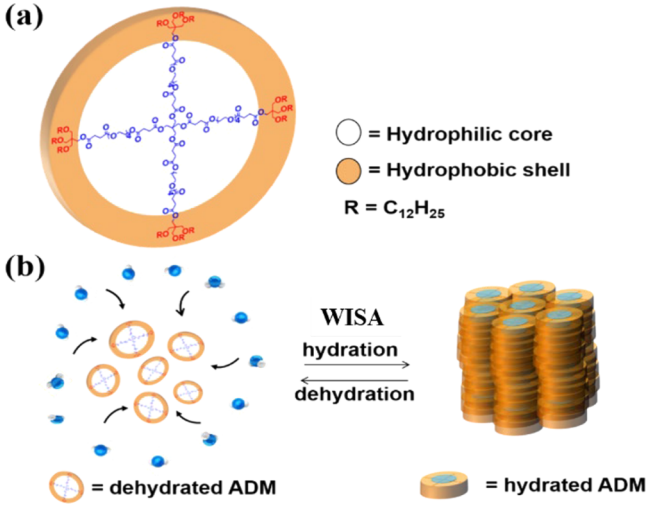

Figure 1. (a) The chemical structures of the ADM. (b) Illustration of the WISA of water and ADM.

was designed for the study. Since the conformational change of the host molecules is an essential step in the induced-fit mechanism, flexible hydrophilic and hydrophobic chains were chosen as the building blocks to provide ADM with high conformation freedom upon interaction with water. Our results show that the WISA of ADM is a kinetic process activated by water. The process results in adaptive artificial water channels (aAWCs) which include water molecules as the coassembly units. In literature, carbon nanotubes (CNTs),[22,23] dendritic dipeptide,[24] imidazole-quartet,[25] and pillar[5]arenes[26−28] aqua-foldamers,[29] have been demonstrated as AWCs that provide water permeability for lipid membranes.[22,30] These molecules form tube-like structures to mimic the pore structure and functions of transmembrane proteins.[31] Nevertheless, their rigid structures prevent water molecules from taking an active role in their self-assembly process. In contrast, the flexibility of ADM allows water to actively govern the assembly/disassembly of ADM *via* fitting into the hydrophilic core of ADM, and to further conduct the WISA process, as illustrated in Figure 1b. Moreover, the dynamic interaction between water and ADM makes water an orientation−directional guest molecule that controls the growth direction of the aAWCs; by incorporating the concept of row nucleation,[32−34] the "directional WISA" method in this study produced the well-aligned and water-permeable aAWC array in the bulk phase. The aAWC array of ADM *via* the directional WISA process shows potential in the membrane application. The water adaptivity of the ADM thus makes water an active substrate that governs the supramolecular chemistry and function of synthetic molecules.

RESULTS AND DISCUSSION

Structural Characterization of ADM. The ADM uses 4 tetra(ethylene glycol) (TEG) chains to form its hydrophilic core and 12 dodecyl chains to form its hydrophobic shell. It was synthesized by connecting four amphiphilic arms to a pentaerythritol core *via* Steglich esterification (Scheme S1). The synthetic details can be found in the Supporting Information, and the ^{1}H NMR, ^{13}C NMR, and mass spectra shown in Figures S1−S7 confirm the chemical identities of the product. The differential scanning calorimetry (DSC) thermograph of ADM (Figure S8a) shows two endothermic phase transitions at −5.17 and 16.5 °C, suggesting that in the heating course, the ADM first transformed into a mesophase at −5.17 °C and then isotropized into an amorphous liquid at 16.5 °C. In Figure 2a, the polarized light optical microscopy (POM)

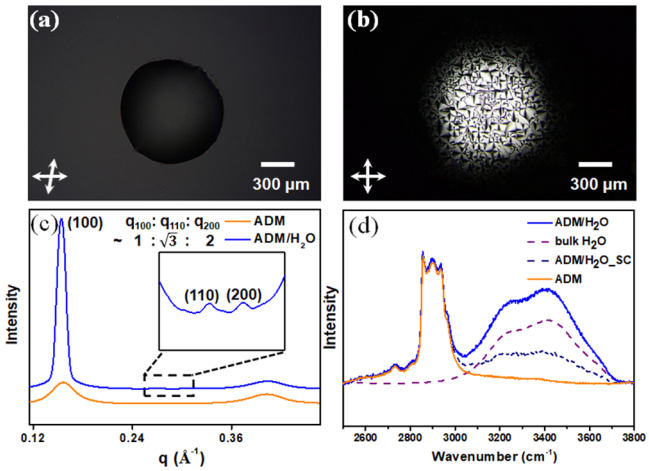

Figure 2. POM micrographs of (a) an ADM droplet and (b) the same droplet covered with water (denoted as the ADM/H_2O sample). (c) SAXS patterns and (d) confocal Raman spectra of the amorphous ADM liquid (orange solid line) and ADM/H_2O (blue solid line). The navy dash line shows the Raman signal of the solute-correlated (SC) water, and purple dash line shows the Raman signal of the solute-uncorrelated (SUC) water in the Col_h of ADM/H_2O, which were deduced from the ADM/H_2O spectrum *via* the HAMAND analysis. In the POM micrographs, the two arrows on the bottom-left indicate the polarization directions of the polarizer and analyzer. In panel a, the polarizer and the analyzer were purposely adjusted away from the cross-polarization, so that the isotropic droplet can be observed.

micrograph of ADM further confirmed that the isotropization temperature (T_i) of the ADM is at 16.5 °C, because at room temperature (26 °C), the ADM is an isotropic liquid that exhibits no birefringence and no texture. However, when water was dropped onto the ADM liquid droplet, the amorphous ADM became birefringent and showed a fan-like texture (Figure 2b). These intriguing phenomena suggest that water can activate the ADM to assemble into an ordered phase. Moreover, as can be seen in Figure S8a (blue trace), the hydration process also elevates the T_i of the ADM from 16.5 to 28.6 °C, indicating that the water-induced self-assembly (WISA) of ADM stabilizes the

https://doi.org/10.1021/acsnano.1c04994
ACS Nano 2021, 15, 14885−14890

mesophase of the hydrated ADM (as illustrated in Figure S8b) to make the mesophase a stable phase at room temperature.

The self-assembly structures of the ADM droplet that was covered with water (denoted as the ADM/H_2O sample) was further characterized by small-angle X-ray scattering (SAXS). The scattering halos in Figure 2c (orange trace) reconfirm that without water, the ADM is an amorphous liquid. When covered with water, ADM/H_2O gave diffraction peaks with a q ratio of $1:\sqrt{3}:2$ (Figure 2c, blue trace), indicating that the ADM and water molecules coassembled into a hexagonal columnar phase (Col_h) with $a = b = 4.69$ nm, $\gamma = 120°$. The presence of water in the Col_h was further characterized by confocal Raman microspectroscopy, which has a space resolution of 2 μm to enable the probe of the Raman signals only within an ADM droplet. Figure 2d shows that the amorphous ADM gave no water signal, but only the CH stretch band at 2800−3000 cm^{-1}, proving that the amorphous ADM is anhydrous. In contrast, the sample ADM/H_2O showed the OH stretch band of water at 3000−3800 cm^{-1} in addition to the CH stretch band of ADM, demonstrating that the Col_h of ADM/H_2O contains interstitial water. Using HAMAND analysis, the signal from water was further analyzed to obtain the contribution from the solute-correlated water (navy dash line) which strongly interacts with the ADM molecules, and the solute-uncorrelated water (purple dash line), which appears to be similar to bulk water.[35,36] The presence of the solute-correlated water further supports the presence of the interstitial water confined within the hydrophobic shell of ADM. The SAXS and Raman data thus confirmed that water molecules activate the self-assembly and coassemble with the ADMs to form the Col_h phase that contains the hexagonally arranged amphiphilic columns as illustrated in Figure 1b. The presence of water is essential for the stability of these amphiphilic columns; once water evaporated from the ADM droplet, the ADM droplet quickly lost its birefringence (see Figure S9). As a result, each amphiphilic column in the Col_h phase can be identified as an individual aAWC that is constructed and destructed through the dynamic interaction between the ADMs and water molecules. The coassembly process can also be considered as the WISA process in which water molecules act as the substrate to activate and participate in the self-assembly of the host molecules, ADMs.

The Essential Noncovalent Interaction in WISA. To identify the essential noncovalent interactions that activate the WISA process, in addition to water, protic solvents, aprotic solvents and ionic aqueous solutions were tested as the chemical effectors of ADM. In Figure 3a−d and Figure S10, the POM micrographs show that the WISA of ADM can also be activated by protic solvents such as ethanol, acetic acid, and diethylamine, but not by the aprotic polar solvents such as *N*,*N*-dimethylmethanamide and dimethyl sulfoxide. These results suggest that the WISA process of ADM requires not only the high polarity of the substrate molecules but also hydrogen bonds to facilitate the formation of the aAWCs. Furthermore, ionic compounds in water were found to hinder water from assembling with the ADM. For instance, Figure 3e,f reveals that when 5 wt % $NaCl_{(aq)}$ solution was dropped onto an ADM droplet, the WISA of ADMs still can work, but the birefringence of the ADM droplet becomes weaker. Continuous increase in the concentration of the $NaCl_{(aq)}$ solution further obstructed and eventually stopped the WISA process when the concentration of the $NaCl_{(aq)}$ solution reached 15 wt %. (The detailed experiment is shown in Figure S11.) It is possible that the increase of salt concentration in water raises the osmotic

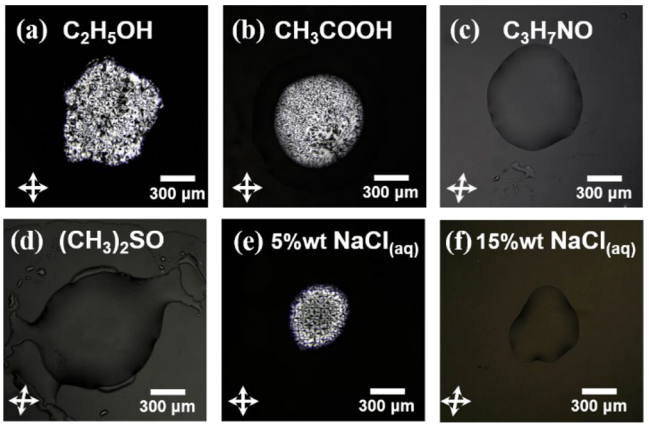

Figure 3. POM micrographs of ADM droplets that were covered with (a,b) protic solvents, (c,d) aprotic solvents, and (e,f) 5 and 15 wt % $NaCl_{(aq)}$ solutions.

pressure of the aqueous solution and enables the high-concentration $NaCl_{(aq)}$ solution to dehydrate ADM, which could consequently cause the collapse of the aAWCs. Nevertheless, since the ADM still carries out WISA with the lower concentration $NaCl_{(aq)}$ solutions (<15 wt %), it shows the ability to extract water from saline solutions, and may be applied as a forward osmosis desalination material in the future.[37]

Growth of a Well-Aligned aAWCs Array *via* WISA. In membrane applications, studies have shown that the morphological control of the water channels in the membranes is a prerequisite for obtaining high water permeability.[38] For the case of ADMs, utilizing WISA, the growth of the well-aligned aAWC array of ADMs is conducted in the apparatus shown in Figure 4a. At the beginning of the experiment, water was placed

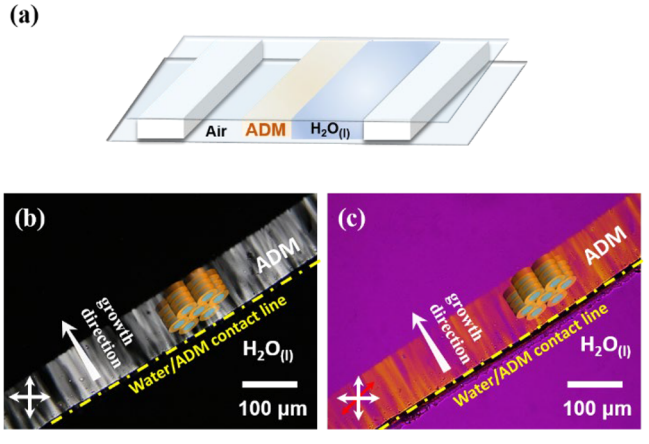

Figure 4. (a) The illustration of experimental apparatus for well-aligned aAWCs growth. The POM micrographs of the well-aligned aAWCs of ADM that were taken (b) w/o and (c) w/the full wavelength retardation plate. The aAWCs of ADM locate at the bright area in panel b and the yellow area in panel c. The red arrow in panel c represents the slow axis of the full wavelength retardation plate.

to the edge of an ADM droplet. At the ADM/$H_2O_{(l)}$ contact line, water acted as an orientation−directional guest molecule. By hydrating ADMs, in Figure 4b, the hydrated ADMs created a row of nuclei to facilitate the unidirectional growth of the aAWCs, which resulted in a "directional WISA" to give the highly oriented array of aAWCs. In Figure 4c, a full-wavelength

https://doi.org/10.1021/acsnano.1c04994
ACS Nano 2021, 15, 14885−14890

retardation plate was used in the POM observation to probe the orientation of the aAWCs. The uniform yellow color from the aAWCs indicates that the long axes of the aAWCs are well-aligned along the growth direction. (Please see Figure S12 for the characterization details and the working principle of the full-wavelength retardation plate.) The channel length of the oriented aAWCs reached over 400 μm (Figure 5a–c) as long

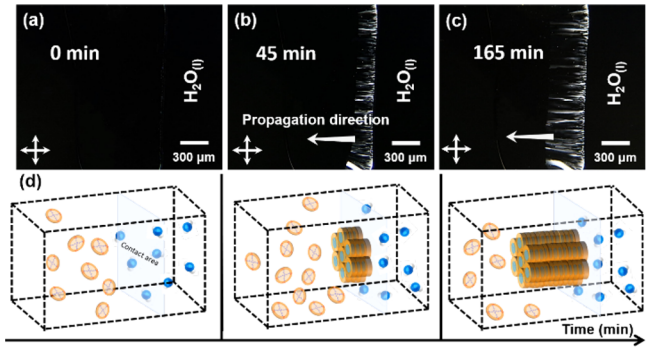

Figure 5. (a–c) POM micrographs of the aligned water channels of ADM at different times after contact with water on the right side. (d) Illustration of the directional WISA.

as the aAWCs could transport water to the front of the channels and further hydrate the ADM to conduct WISA at the interface of the aAWCs and isotopic liquid, as illustrated in Figure 5d.

Water Governs the Permeability of ADM. The water permeability of the well-aligned aAWC array was further characterized by the apparatus illustrated in Figure 6a. The

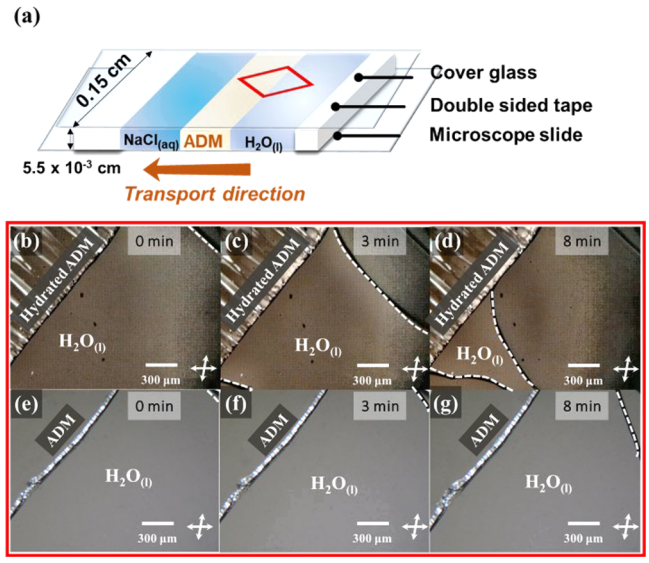

Figure 6. (a) Illustration of the $NaCl_{(aq)}$/ADM/$H_2O_{(l)}$ sandwich-type apparatus. The red frame indicates the region where the OM micrographs in panels b–g were taken. Water transport experiment (0–8 min) of the (b–d) aAWC array and (e–g) ADM isotropic liquid. The white dash line is labeled as the water edge.

oriented aAWC array was first grown in the apparatus as shown in Figure 4a, and a 0.5 wt % $NaCl_{(aq)}$ solution was then injected at the left side of an aAWCs array. The sandwich configuration of $NaCl_{(aq)}$/aAWC array/$H_2O_{(l)}$ generates osmotic pressure that enables the aAWCs to deliver $H_2O_{(l)}$ toward the $NaCl_{(aq)}$ side. Therefore, $H_2O_{(l)}$ at the right side is drained through the aAWCs as shown in Figure 6b–d. However, when the same experiment was done on an ADM isotropic liquid, the water transport was only negligible (Figure 6e–g). Since the contact area (A_c) between $H_2O_{(l)}$ and ADM is known to be 8.25×10^{-4} cm^2 (height, 5.5×10^{-3} cm; width, 0.15 cm, see Figure 6a) and the draining rate of $H_2O_{(l)}$ (R_{H2O}, mL s^{-1}) can be recorded under the OM (Figure 6b–d), the water permeability of the oriented aAWC array of ADM (P_{ADM}, mL s^{-1} cm^{-2}) was roughly estimated according to eq 1.

$$P_{ADM} = R_{H2O}/A_c \quad (1)$$

For the oriented aAWC array of ADM, the averaged R_{H2O} was measured as 9.08×10^{-9} mL s^{-1} (averaged out of 5 times of measurements), so the P_{ADM} was then calculated as 1.10×10^{-5}mL s^{-1} cm^{-2}. In contrast, the water permeability of the isotropic ADM liquid is negligible (Figure 6e–g), confirming again that the formation of well-oriented aAWCs is essential for ADM to perform water transport. These results showed that the ADM requires water to initiate the formation of its well-oriented structure to active its function, and water can regulate both the self-assembly and function of synthetic molecules as it does those of natural materials.

CONCLUSIONS

In this study, water was used as an active chemical effector to regulate the WISA and function of an ADM. Characterization results confirmed that water molecules and the ADM coassemble into a Col_h phase that contains aAWCs. Removal of water causes the destruction of the aAWCs, which confirms the dynamic characteristics of aAWCs. Utilizing the dynamic characteristics of the aAWCs, a well-aligned aAWC array was prepared *via* directional WISA where water was used as orientation–directional guest molecules. Since the aAWC array can transport water but the dehydrated ADM cannot, water acts as an active substrate to activate the self-assemble of the ADM for the water transportation.

EXPERIMENTAL SECTION

Materials. 4-(Dimethylamino)pyridinium 4-toluenesulfonate (DPTS) was prepared according to a literature procedure.[39] All other reagents and solvents were purchased from commercial sources and were used without purification. ^1H and ^{13}C nuclear magnetic resonance (NMR) spectra were recorded on an Agilent Unity-400 NMR spectrometer (400 MHz for ^1H, 101 MHz for ^{13}C), using $CDCl_3$ as d-solvents to identify the molecular structures at 25 °C. The field desorption ionization mass spectrometry (FD-mass) was recorded on JEOL Accu TOF FCX to show the molecular weight of ADM.

Polarizing Optical Microscope (POM). Optical microscopy (OM) and polarizing optical microscopy (POM) images were recorded by a Leica DM2700 optical microscopy. A full wavelength retardation plate was applied to the POM observation of the aligned adaptive artificial water channels (aAWCs) at ambient conditions. The full wavelength retardation plate is a thin transparent crystal that owns birefringence.

Differential Scanning Calorimetry (DSC). DSC results were obtained by a TA Instruments Q series 20 with RSC 90 cooling system to provide a low temperature environment. Nitrogen was used as purge gas, and samples were scanned from −40 to 80 °C. The measurements operated three cycles at a scan rate of 10 °C min^{-1}.

Small-Angle X-ray Scattering (SAXS). SAXS measurements were recorded at 23A beamline of national synchrotron radiation research center (NSRRC) in Taiwan. The ring energy of NSRRC was operated at 15 keV with a typical current of 300 mA. The wavelength of the X-rays was 0.827 Å and the distance was 3168.67 mm between samples and detectors to give a q range of 0.006 to 0.42 $Å^{-1}$. q is the scattering

https://doi.org/10.1021/acsnano.1c04994
ACS Nano 2021, 15, 14885–14890

vector, related to the scattering angle (2θ) and the photon wavelength (λ) by $q = 4\pi \sin(\theta)/\lambda$.

Raman Spectroscopy. A lab-built confocal Raman microspectrometer with the following components was used for the measurements. The second harmonic (532 nm) of a CW Nd:YVO_4 laser (Verdi-V5, Coherent) was used as the excitation source. A small part of the output was used with a high-resolution wavelength meter (WS-7, HighFinesse) to monitor and stabilize the laser wavelength. The excitation beam passed a laser line filter and a linear polarizer (Glan Taylor prism) and was directed by a beam splitter (10R:90T) into an inverted microscope (*iX71*, Olympus). The laser beam was focused inside the sample chamber using a 40× objective lens (LUCPlanFLN 40X/NA = 0.60/air, Olympus). Typical laser power was 0.41 mW for the samples which were placed in a bottom dish. Backscattered light passed through the beam splitter and was focused by a lens on a 100 μm pinhole, followed by another lens forming a collimated beam. Three volume Bragg-notch filters (OptiGrate) were used to remove the Rayleigh scattering. After Rayleigh rejection, the light was focused on the spectrometer slit (slit width = 100 μm) using an achromatic convex lens. The scattered light was dispersed by a polychromator (f = 50 cm, f/6.5; *SP-2500i*, Princeton Instruments) and detected by a Peltier-cooled CCD detector (*Andor Newton, 970P*).

HAMAND Analysis. HAMAND (Hypothetical Addition Multivariate Analysis with Numerical Differentiation) combines the principle of the standard addition method with two-component MCR-ALS (multivariate curve resolution with alternating least-squares) technique. It is a numerical chemometric method for separating and quantifying the known target spectral component(s) from a complex spectrum. HAMAND processes a number of numerically generated hypothetical model spectra (S_j) that are obtained by adding the standard spectrum (S_{std}) to the spectra of the unknown sample (S_{unkn}) with different coefficients (c_j):

$$S_j = S_{unkn} + c_j S_{std} \quad (2)$$

Subsequently, these hypothetical spectra are separated into two spectral, components W_1 (the spectrum corresponding to all the other substances except for the target) and W_2 (the target spectrum) with intensity profiles of H_1 (constant) and H_2 (linearly dependent on hypothetically added coefficient representing concentration (c_j) by using a simple two-component MCR-ALS. The calibration line which is obtained by plotting the intensity profile H_2 versus a hypothetically added coefficient determines the amount of the target spectrum already contained in the sample. Here, Raman spectrum of pure water was used as the S_{std}, with the Raman spectrum of ADM/H_2O as S_{unkn} to obtain the residual spectrum, W_1, which is regarded as the solute-correlated (SC) spectrum of water.

The synthetic details, ^{1}H NMR, ^{13}C NMR, and mass spectra of the ADM can be found in the Supporting Information.

ASSOCIATED CONTENT

Supporting Information

The Supporting Information is available free of charge at https://pubs.acs.org/doi/10.1021/acsnano.1c04994.

Detailed synthesis, structural characterization methods and analyses (PDF)

AUTHOR INFORMATION

Corresponding Author

Chien-Lung Wang − *Department of Applied Chemistry, National Yang Ming Chiao Tung University, Hsinchu 30010, Taiwan;* orcid.org/0000-0002-5977-2836; Email: kclwang@nctu.edu.tw

Authors

Hsi-Yen Chang − *Department of Applied Chemistry, National Yang Ming Chiao Tung University, Hsinchu 30010, Taiwan*

Kuan-Yi Wu − *National Synchrotron Radiation Research Center, Hsinchu 30076, Taiwan*

Wei-Chun Chen − *Department of Applied Chemistry, National Yang Ming Chiao Tung University, Hsinchu 30010, Taiwan*

Jing-Ting Weng − *Department of Applied Chemistry, National Yang Ming Chiao Tung University, Hsinchu 30010, Taiwan*

Chin-Yi Chen − *Department of Applied Chemistry, National Yang Ming Chiao Tung University, Hsinchu 30010, Taiwan*

Ankit Raj − *Department of Applied Chemistry, National Yang Ming Chiao Tung University, Hsinchu 30010, Taiwan*

Hiro-o Hamaguchi − *Department of Applied Chemistry, National Yang Ming Chiao Tung University, Hsinchu 30010, Taiwan*

Wei-Tsung Chuang − *National Synchrotron Radiation Research Center, Hsinchu 30076, Taiwan;* orcid.org/0000-0002-9000-2194

Xiaosong Wang − *Department of Chemistry, Waterloo Institute for Nanotechnology, University of Waterloo, Waterloo, Ontario N2L 3G1, Canada;* orcid.org/0000-0002-6415-4768

Complete contact information is available at: https://pubs.acs.org/10.1021/acsnano.1c04994

Author Contributions

$^{\perp}$H.-Y.C. and K.-Y.W. contributed equally to this work.

Notes

The authors declare no competing financial interest.

ACKNOWLEDGMENTS

This work is supported by the Ministry of Science and Technology, Taiwan (MOST 109-2223-E-009-001-MY3). The authors thank the staff at the National Synchrotron Radiation Center for their support in carrying out the structural characterizations.

REFERENCES

(1) Jensen, M. Ø.; Borhani, D. W.; Lindorff-Larsen, K.; Maragakis, P.; Jogini, V.; Eastwood, M. P.; Dror, R. O.; Shaw, D. E. Principles of Conduction and Hydrophobic Gating in K^+ Channels. *Proc. Natl. Acad. Sci. U. S. A.* **2010**, *107*, 5833−5838.

(2) Oroguchi, T.; Nakasako, M. Changes in Hydration Structure Are Necessary for Collective Motions of a Multi-Domain Protein. *Sci. Rep.* **2016**, *6*, 1−14.

(3) Rao, S.; Lynch, C. I.; Klesse, G.; Oakley, G. E.; Stansfeld, P. J.; Tucker, S. J.; Sansom, M. S. Water and Hydrophobic Gates in Ion Channels and Nanopores. *Faraday Discuss.* **2018**, *209*, 231−247.

(4) Rini, J. M.; Schulze-Gahmen, U.; Wilson, I. A. Structural Evidence for Induced Fit as a Mechanism for Antibody-Antigen Recognition. *Science* **1992**, *255*, 959−965.

(5) Koshland Jr, D. E. The Key−Lock Theory and the Induced Fit Theory. *Angew. Chem., Int. Ed. Engl.* **1995**, *33*, 2375−2378.

(6) Hammes, G. G.; Chang, Y.-C.; Oas, T. G. Conformational Selection or Induced Fit: A Flux Description of Reaction Mechanism. *Proc. Natl. Acad. Sci. U. S. A.* **2009**, *106*, 13737−13741.

(7) Gorga, F. R.; Lienhard, G. E. Equilibriums and Kinetics of Ligand Binding to the Human Erythrocyte Glucose Transporter. Evidence for an Alternating Conformation Model for Transport. *Biochemistry* **1981**, *20*, 5108−5113.

(8) Vidaver, G. A. Inhibition of Parallel Flux and Augmentation of Counter Flux Shown by Transport Models Not Involving a Mobile Carrier. *J. Theor. Biol.* **1966**, *10*, 301−306.

(9) Beckstein, O.; Tai, K.; Sansom, M. S. Not Ions Alone: Barriers to Ion Permeation in Nanopores and Channels. *J. Am. Chem. Soc.* **2004**, *126*, 14694−14695.

(10) Oka, Y.; Asano, T.; Shibasaki, Y.; Lin, J.-L.; Tsukuda, K.; Katagiri, H.; Akanuma, Y.; Takaku, F. C-terminal Truncated Glucose Transporter is Locked into an Inward-Facing Form without Transport Activity. *Nature* **1990**, *345*, 550−553.
(11) Beckstein, O.; Sansom, M. S. The Influence of Geometry, Surface Character, and Flexibility on the Permeation of Ions and Water through Biological Pores. *Phys. Biol.* **2004**, *1*, 42.
(12) Cram, D. J.; Cram, J. M. Host-Guest Chemistry. *Science* **1974**, *183*, 803−809.
(13) Lehn, J.-M. From Supramolecular Chemistry towards Constitutional Dynamic Chemistry and Adaptive Chemistry. *Chem. Soc. Rev.* **2007**, *36*, 151−160.
(14) Miyata, K.; Nishiyama, N.; Kataoka, K. Rational Design of Smart Supramolecular Assemblies for Gene Delivery: Chemical Challenges in the Creation of Artificial Viruses. *Chem. Soc. Rev.* **2012**, *41*, 2562−2574.
(15) Lehn, J.-M. Perspectives in Chemistry − Steps towards Complex Matter. *Angew. Chem., Int. Ed.* **2013**, *52*, 2836−2850.
(16) Lehn, J. M. Perspectives in Chemistry − Aspects of Adaptive Chemistry and Materials. *Angew. Chem., Int. Ed.* **2015**, *54*, 3276−3289.
(17) Lutz, J.-F.; Lehn, J.-M.; Meijer, E.; Matyjaszewski, K. From Precision Polymers to Complex Materials and Systems. *Nat. Rev. Mater.* **2016**, *1*, 1−14.
(18) Wang, A.; Shi, W.; Huang, J.; Yan, Y. Adaptive Soft Molecular Self-Assemblies. *Soft Matter* **2016**, *12*, 337−357.
(19) Krieg, E.; Rybtchinski, B. Noncovalent Water-Based Materials: Robust yet Adaptive. *Chem. - Eur. J.* **2011**, *17*, 9016−9026.
(20) Biedermann, F.; Nau, W. M.; Schneider, H. J. The Hydrophobic Effect Revisited—Studies with Supramolecular Complexes Imply High-Energy Water as a Noncovalent Driving Force. *Angew. Chem., Int. Ed.* **2014**, *53*, 11158−11171.
(21) Jordan, J. H.; Gibb, B. C. Molecular Containers Assembled through the Hydrophobic Effect. *Chem. Soc. Rev.* **2015**, *44*, 547−585.
(22) Holt, J. K.; Park, H. G.; Wang, Y.; Stadermann, M.; Artyukhin, A. B.; Grigoropoulos, C. P.; Noy, A.; Bakajin, O. J. S. Fast Mass Transport through Sub-2-Nanometer Carbon Nanotubes. *Science* **2006**, *312*, 1034−1037.
(23) Tsarfati, Y.; Strauss, V.; Kuhri, S.; Krieg, E.; Weissman, H.; Shimoni, E.; Baram, J.; Guldi, D. M.; Rybtchinski, B. Dispersing Perylene Diimide/SWCNT Hybrids: Structural Insights at the Molecular Level and Fabricating Advanced Materials. *J. Am. Chem. Soc.* **2015**, *137*, 7429−7440.
(24) Kaucher, M. S.; Peterca, M.; Dulcey, A. E.; Kim, A. J.; Vinogradov, S. A.; Hammer, D. A.; Heiney, P. A.; Percec, V. Selective Transport of Water Mediated by Porous Dendritic Dipeptides. *J. Am. Chem. Soc.* **2007**, *129*, 11698−11699.
(25) Le Duc, Y.; Michau, M.; Gilles, A.; Gence, V.; Legrand, Y. M.; van der Lee, A.; Tingry, S.; Barboiu, M. Imidazole-Quartet Water and Proton Dipolar Channels. *Angew. Chem., Int. Ed.* **2011**, *50*, 11540−11540.
(26) Si, W.; Chen, L.; Hu, X. B.; Tang, G.; Chen, Z.; Hou, J. L.; Li, Z. T. Selective Artificial Transmembrane Channels for Protons by Formation of Water Wires. *Angew. Chem., Int. Ed.* **2011**, *50*, 12564−12568.
(27) Si, W.; Xin, P.; Li, Z.-T.; Hou, J.-L. Tubular Unimolecular Transmembrane Channels: Construction Strategy and Transport Activities. *Acc. Chem. Res.* **2015**, *48*, 1612−1619.
(28) Barboiu, M. Artificial Water Channels−Incipient Innovative Developments. *Chem. Commun.* **2016**, *52*, 5657−5665.
(29) Shen, J.; Ye, R.; Romanies, A.; Roy, A.; Chen, F.; Ren, C.; Liu, Z.; Zeng, H. Aquafoldmer-Based Aquaporin-Like Synthetic Water Channel. *J. Am. Chem. Soc.* **2020**, *142*, 10050−10058.
(30) Shen, Y.-x.; Song, W.; Barden, D. R.; Ren, T.; Lang, C.; Feroz, H.; Henderson, C. B.; Saboe, P. O.; Tsai, D.; Yan, H.; Butler, P. J.; Bazan, G. C.; Phillip, W. A.; Hickey, R. J.; Cremer, P. S.; Vashisth, H.; Kumar, M. Achieving High Permeability and Enhanced Selectivity for Angstrom-Scale Separations Using Artificial Water Channel Membranes. *Nat. Commun.* **2018**, *9*, 1−11.
(31) Agre, P. Aquaporin Water Channels. *Angew. Chem., Int. Ed.* **2004**, *43*, 4278−4290.
(32) Hobbs, S. Row Nucleation of Isotactic Polypropylene on Graphite Fibres. *Nature, Phys. Sci.* **1971**, *234*, 12−13.
(33) Wu, K. Y.; Wu, T. Y.; Chang, S. T.; Hsu, C. S.; Wang, C. L. A Facile PDMS-Assisted Crystallization for the Crystal-Engineering of C60 Single-Crystal Organic Field-Effect Transistors. *Adv. Mater.* **2015**, *27*, 4371−4376.
(34) Chen, J.; Zhu, E.; Liu, J.; Zhang, S.; Lin, Z.; Duan, X.; Heinz, H.; Huang, Y.; De Yoreo, J. J. Building Two-Dimensional Materials One Row at a Time: Avoiding the Nucleation Barrier. *Science* **2018**, *362*, 1135−1139.
(35) Davis, J. G.; Gierszal, K. P.; Wang, P.; Ben-Amotz, D. Water Structural Transformation at Molecular Hydrophobic Interfaces. *Nature* **2012**, *491*, 582−585.
(36) Ando, M.; Lednev, I. K.; Hamaguchi, H.-o. Quantitative Spectrometry of Complex Molecular Systems by Hypothetical Addition Multivariate Analysis with Numerical Differentiation (HAMAND). *Frontiers and Advances in Molecular Spectroscopy* **2018**, 369−378.
(37) Klaysom, C.; Cath, T. Y.; Depuydt, T.; Vankelecom. Forward and Pressure Retarded Osmosis: Potential Solutions for Global Challenges in Energy and Water Supply. *Chem. Soc. Rev.* **2013**, *42*, 6959−6989.
(38) Feng, X.; Kawabata, K.; Cowan, M. G.; Dwulet, G. E.; Toth, K.; Sixdenier, L.; Haji-Akbari, A.; Noble, R. D.; Elimelech, M.; Gin, D. L.; Osuji, C. O. Single Crystal Texture by Directed Molecular Self-Assembly along Dual Axes. *Nat. Mater.* **2019**, *18*, 1235−1243.
(39) Moore, J. S.; Stupp, S. I. Room Temperature Polyesterification. *Macromolecules* **1990**, *23*, 65−70.

https://doi.org/10.1021/acsnano.1c04994
ACS Nano 2021, 15, 14885−14890